# New evidence for the idea of timescale invariance of relaxation processes in simple liquids: the case of molten sodium

**R M Yulmetyev[1], A V Mokshin[1], T Scopigno[2] and P Hänggi[3]**

[1] Department of Physics, Kazan State Pedagogical University, Kazan, Mezhlauk 1, 420021, Russia
[2] Dipartimento di Fisica and INFM, Universitá di Roma 'La Sapienza', I-00185 Roma, Italy
[3] Department of Physics, University of Augsburg, Universitätsstrasse 1, D-86135 Augsburg, Germany

E-mail: rmy@dtp.ksu.ras.ru, mav@dtp.ksu.ras.ru and tullio.scopigno@phys.uniroma1.it

**Abstract**

The idea of the timescale invariance of relaxation processes in liquids (Yulmetyev *et al* 2001 *Phys. Rev.* E **64** 057101; 2002 *JETP Lett.* **76** 147) is used to analyse the short-wave collective excitation in liquid sodium, as recently measured by means of very-high-energy-resolution inelastic x-ray scattering (Scopigno *et al* 2002 *Phys. Rev.* E **65** 031205). The dynamic structure factor, $S(Q, \omega)$, calculated on the basis of this idea is in very good agreement with the experimental data in the wavevector range from 1.5 to 14.6 $nm^{-1}$, where pronounced collective excitations exist. The frequency dependence of the non-Markovity parameter $\epsilon_i(Q, \omega)$ $(i = 1, 2, 3, 4)$ allows us to reveal the alternation of the amplification and the decay of non-Markovity effects for the observed region of wavevector $Q$.

## 1. Introduction

The study of the nature of the high-frequency collective excitations in atomic and molecular aggregates belongs to one of the most fundamental problems of condensed matter physics. Whereas the properties of these excitations are quite well understood in crystals, many aspects are still largely unknown at present as far as disordered systems are concerned. Among these latter, liquid metals plays a crucial role, as they exhibit pronounced inelastic features in the terahertz frequency region.

Until now valuable information on the dynamical properties of liquid metals was mainly received with the help of inelastic neutron scattering (INS) experiments [1, 2], a method that allows one to measure the frequency spectrum of the density fluctuations in a wide range of wavevector values and frequencies. The possibility of using x-rays for inelastic scattering

by collective excitations has been attractive for a long time because of the complementary advantages and drawbacks of this technique in comparison to INS. Nevertheless, the necessity of a much higher resolving power prevented the parallel development of the two methods. Many efforts have been made in the last 20 years to increase the global efficiency of inelastic x-ray scattering (IXS) experiments [3] and, recently, the availability of the third generation of x-ray sources, together with a great technological impulse, allowed us to bring IXS resolutions in this millielectronvolt energy range with scattering rates closer to INS ones [4]. In the specific case of liquid metals, these experimental studies have been recently reported on liquid lithium [5, 6] and aluminium [7], sodium [8–10], germanium [11], mercury [12] and gallium [13].

A very useful tool, complementary to the 'traditional' experimental facilities, is provided by numeric experiments, molecular dynamics (MD) simulation in particular. This method allows one to investigate both the single-particle and the collective dynamics of liquids on the basis of a suitable interatomic potential. As an example of such studies performed in liquid metals, one can refer to MD results for liquid lithium at 470 and 843 K [14], and also the recent MD simulation of liquid lithium near the melting temperature [15].

The mechanisms of relaxation processes, connected with the collective excitations both in hydrodynamic and in microscopic areas about one to two interatomic distances, have been well established with the help of numerical simulation, and recently detailed information on the relaxation processes has been obtained by experimental IXS data [6, 13]. However, many aspects of the physical origin of the relaxation processes in microscopic areas of liquid metals still remain unclear.

The area of the measured values of wavevector $Q$ in INS and IXS of liquid metals is usually bounded by a 'low-$Q$' region where the dynamic structure factor $S(Q, \omega)$ consists of the central peak at $\omega = 0$ and two side peaks at $\omega \neq 0$, and a 'high-$Q$' region where the dynamic structure factor has only a single, Gaussian, peak [1, 6]. The majority of the advanced theories fully correspond to the experimental data at high values of $Q$. However, in the regions of wavevectors $Q$ where $S(Q, \omega)$ has a triple-peak structure, significant difference between the appropriate theories and the experiments is observed (see, for example, [16]).

In some recent works [6, 7, 9, 10], it has been shown that a simple viscoelastic approach with a single decay time does not account for the spectral features of simple liquid metals. Indeed, to reproduce the dynamic structure factor in these systems, three relevant timescales must be invoked, two of them associated with viscous processes and one with the thermal coupling between density and temperature fluctuations.

In the present work we develop a theory, universal for the whole area of values of wavevectors, based on one of the most fundamental ideas of modern physics and mathematics: scale invariance. The experimentally observed relaxation process (in particular, for density fluctuations) is the result of a multilevel chain of interconnected relaxation processes. However, the experiment only enables us to observe and estimate a single relaxation process of the whole set. Now, on a certain relaxation level, an invariance (equiscaling) of the nearest interconnected relaxation processes can exist, and the relaxation time $\tau$ is a convenient physical measure of such an invariance. The characteristic values of the set of relaxation times essentially depend on the certain level of relaxation, while the features of this level determine both the number and the properties of the timescales, through which all the microdynamics is expressed. Thus, the number of these timescales can be three, two and even one depending on the concrete structural features of the studied metal, values of wavevector $Q$ etc. A similar approach was presented first in our previous work [17], where the relaxation processes in liquid caesium were investigated. The dynamic structure factor $S(Q, \omega)$, calculated on the basis of the advanced theory, was found to agree with experimental data on liquid caesium [2]. The calculation of the physical parameter of non-Markovity $\epsilon_i(Q, \omega)$, which was entered earlier in [18, 19], has

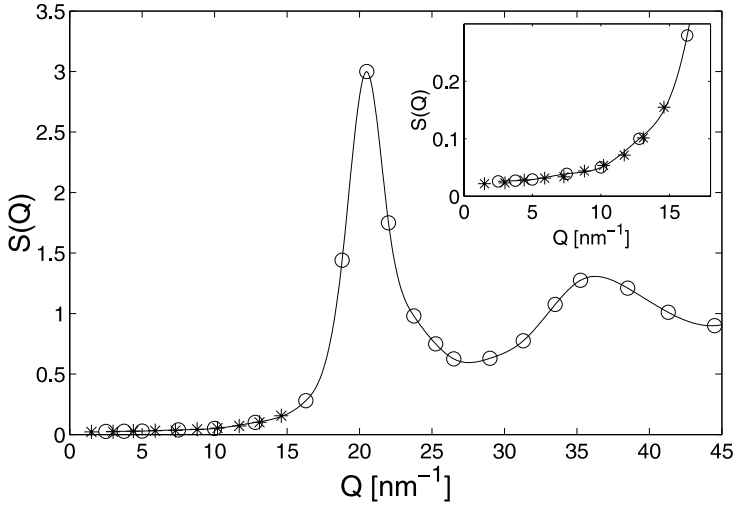


**Figure 1.** Values of the static structure factor $S(Q)$ of liquid sodium from [9] (∗) for the 'low-$Q$' region and from experimental data of Waseda [50] (○).

allowed us to reveal a non-Markov nature of high-frequency collective excitations, shown in side peaks of the dynamic structure factor $S(Q, \omega)$ of liquid caesium in the wavevector range $Q$ from 0.4 up to 1 Å. Obviously, a similar study on other alkaline metals would be useful and interesting to support the above-mentioned scenario.

In this work, we report the results of the dynamic structure factor investigation of liquid sodium near its melting point ($T = 390$ K) for the 'low-$Q$' region from 1.5 to 14.6 nm$^{-1}$ (see figure 1). The layout of the paper is as follows. Section 2 contains the experimental details of a recent very-high-resolution determination of $S(Q, \omega)$. In section 3 we present our theory. The results obtained and discussions are presented in section 4. The conclusion is given in section 5.

## 2. The experiment

The dynamic structure factor of liquid sodium has been recently measured by means of a very-high-resolution inelastic x-ray scattering experiment performed at the beamline ID 28 of the European Synchrotron Radiation Facility (ESRF). The adiabatic sound velocity in this system is about 2500 m s$^{-1}$, a value that is high enough to prevent an extended determination by INS of the $S(Q, \omega)$ in the 'low-$Q$' region where collective excitations exists and propagates with an almost linear dispersion. Moreover, the coherent and incoherent cross sections are almost equivalent in the sodium case, a condition that poses an additional limit for an accurate study of the collective microdynamics only.

In fact, up to a few years ago, the only appropriate technique to study the atomic dynamics at a microscopic level, i.e. in a wavevector region comparable to the inverse mean interatomic distances, was neutrons. In the last decade this situation has gradually changed and the advent of inelastic x-ray scattering has allowed us to perform inelastic experiments with photons [3]. Nevertheless, the development of this technique was prevented at the beginning due to the severe resolution demand necessary to separate excitations of the order of a few millielectronvolts from the energy of the incoming beam (some kiloelectronvolts). Only in

the recent past, thanks to the rapid development of the third-generation sources, have suitable resolutions been achieved [4].

Liquid sodium, together with lithium and the other light metallic elements, has been shown to exhibit inelastic features well above the $Q$ position of the structure factor maximum, with well defined high-frequency modes of propagating nature [8]. The performance of IXS is nowadays very close to the intrinsic theoretical limitations of the technique, both in terms of efficiency and resolution, that has come down to 1 meV, a value that allows one to go beyond the mere determination of the sound speed and attenuation properties. As consequence, one can now use the information contained in all the spectral features in order to test different theoretical models and approaches [9, 10], and this is the aim of the present paper.

The IXS data reported here relate to an experiment that has been performed at fixed exchanged wavevector over a $Q$-region below the first sharp diffraction peak (1.5–15 $\mathrm{nm}^{-1}$) with a $Q$-resolution of $\Delta Q = 0.4\ \mathrm{nm}^{-1}$ full width at half maximum (FWHM). Energy scans in the range $-50 < \mathrm{E} < 50$ meV were collected utilizing the (11 11 11) reflection of the silicon monochromator and analysers for a total energy resolution of $\Delta E = 1.5$ meV FWHM. Each scan took about 300 min; several scans were summed up to 500 s of integration per point. For each scan, five different values of $Q$ could simultaneously be measured thanks to a multiple analyser bench, operating in horizontal scattering geometry. The sample, a high-purity sodium bar, was purchased by Goodfellow. A sample environment similar to the one adopted in previous experiments performed on liquid lithium [6] has been utilized, i.e. an austenitic steel cell heated by a resistor connected to a voltage regulated supply and kept in thermal contact with the cell. The sample length has been chosen in order to match the absorption length of sodium at the working energy 21 747 eV (corresponding to the Si (11 11 11) reflection in backscattering geometry) that is about 5 mm. In fact, this condition maximizes the efficiency of an IXS sample [9].

In figure 2, we report the measured coherent dynamic structure factor at different $Q$ values. Since the incident flux on the sample varies with time, and the five analysers have different scattering efficiencies $E(Q)$, in order to extract the $\tilde{S}(Q, \omega)$ from the raw experimental spectra the data need to be put in absolute units first. A reliable procedure to do this is to make use of the lower-order sum rules holding for the dynamic structure factor in formulae (the suffix $q$ indicates here the true quantum dynamic structure factor, to distinguish it from its classical representation):

$$\Omega_{S_q}^{(0)} = \int \mathrm{d}\omega\, S_q(Q, \omega) = S_q(Q) \tag{1}$$

$$\Omega_{S_q}^{(1)} = \int \mathrm{d}\omega\, S_q(Q, \omega)\omega = \frac{\hbar Q^2}{2M}. \tag{2}$$

Indeed, the experimental spectra, $I(Q, \omega)$, being proportional to the convolution of the scattering law $S_q(Q, \omega)$ with the resolution $R(\omega)$,

$$I(Q, \omega) = E(Q) \int \mathrm{d}\omega'\, S_q(Q, \omega') R(\omega - \omega') \tag{3}$$

in terms of the first two spectral moments of $I$ and $R$, $\Omega_I^{(0)}$, $\Omega_I^{(1)}$, $\Omega_R^{(0)}$ and $\Omega_R^{(1)}$, it holds that

$$S_q(Q) = \frac{\hbar Q^2}{2M} (\Omega_I^{(1)}/\Omega_I^{(0)} - \Omega_R^{(1)}/\Omega_R^{(0)})^{-1}. \tag{4}$$

The normalized spectra (still affected by the resolution broadening) will now be

$$I_N(Q, \omega) = \frac{S_q(Q)}{\int I(Q, \omega\, \mathrm{d}\omega)} I(Q, \omega). \tag{5}$$

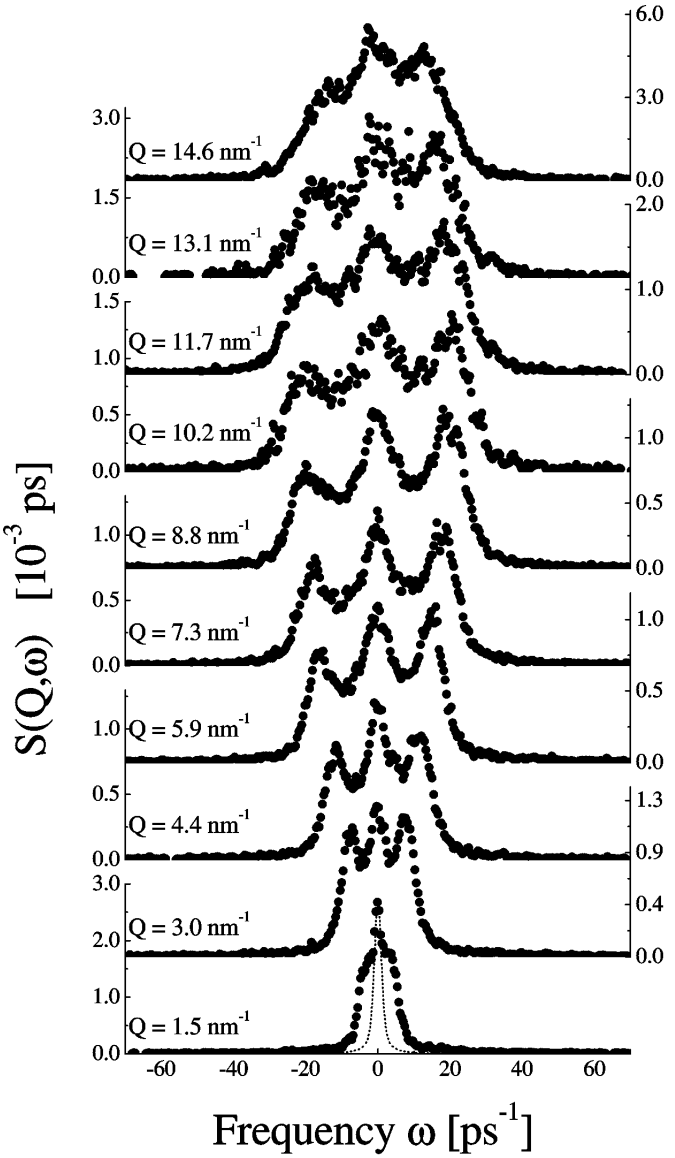


**Figure 2.** Coherent dynamic structure factor of sodium at the melting point as measured by constant $Q$ IXS energy scan (●). The dotted curves indicate the instrumental resolution.

## 3. Theoretical formalism

### *3.1. Fundamentals*

We shall consider here the fluctuations of the local density of $N$ particles in liquid as a dynamic variable:

$$\delta\rho_Q(t) = \frac{1}{V}\sum_{j=1}^{N} e^{iQ\cdot r_j(t)} - \delta_{Q,0}\frac{N}{V}, \tag{6}$$

where $V$ is the volume of the system, $r_j(t)$ is the radius-vector of the $j$th particle at the time moment $t$ and $\delta_{Q,0}$ is Kronecker's symbol.

The normalized time correlation function (TCF) of local-density fluctuations $\delta\rho_Q(t)$ is

$$F(Q,t) = \frac{\langle \delta\rho_Q^*(0)\mathrm{e}^{\mathrm{i}Lt}\delta\rho_Q(0)\rangle}{\langle|\delta\rho_Q(0)|^2\rangle}. \tag{7}$$

It is now possible to construct the infinite chain of connected non-Markov kinetic equations with the help of the Zwanzig–Mori projection operator technique [20, 21]

$$\begin{aligned}
\frac{\mathrm{d}F(Q,t)}{\mathrm{d}t} &= -\Omega_1^2\int_0^t \mathrm{d}\tau\, M_1(Q,\tau)F(Q,t-\tau),\\
\frac{\mathrm{d}M_1(Q,t)}{\mathrm{d}t} &= -\Omega_2^2\int_0^t \mathrm{d}\tau\, M_2(Q,\tau)M_1(Q,t-\tau),\ldots,\\
\frac{\mathrm{d}M_i(Q,t)}{\mathrm{d}t} &= -\Omega_{i+1}^2\int_0^t \mathrm{d}\tau\, M_{i+1}(Q,\tau)M_i(Q,t-\tau).
\end{aligned} \tag{8}$$

Here $L$ is the Liouville operator, $\Omega_1^2, \Omega_2^2, \ldots, \Omega_i^2$ are general relaxation parameters with the dimension of the square of frequency, and $M_i(k,t)$ is the memory function (MF) of the $i$th order. The first frequency parameter $\Omega_1$ is given by the following relation:

$$\Omega_1^2 = k_B T Q^2/mS(Q). \tag{9}$$

Similar expressions for calculation of $\Omega_i^2$, where $i = 2, 3, \ldots$, are also well known, and these relaxation frequency parameters can be expressed in terms of the pair distribution function $g(r)$ and of the higher-order distribution functions.

The Laplace transform of $F(Q,t)$

$$\tilde{F}(Q,z) = \int_0^\infty \mathrm{d}t\, \mathrm{e}^{-zt}F(Q,t)$$

is connected with the scattering function $S(Q,\omega)$ by the following:

$$S(Q,\omega) = \frac{S(Q)}{\pi}\lim_{\epsilon\to+0}\mathrm{Re}[\tilde{F}(Q,\mathrm{i}\omega+\epsilon)]. \tag{10}$$

Here symbol Re means the real part; $S(Q)$ is the static structure factor and the zero-frequency moment of $S(Q,\omega)$ which is defined by

$$S(Q) = \int_{-\infty}^\infty S(Q,\omega)\,\mathrm{d}\omega. \tag{11}$$

Thus, the static structure factor $S(Q)$ is defined by the integral of the coherent scattering law over all energy transfers at constant $Q$ [22]. In the general case frequency moments of the dynamic structure factor are expressed as the following:

$$\omega^{(m)}(Q) = \int_{-\infty}^\infty \omega^m S(Q,\omega)\,\mathrm{d}\omega. \tag{12}$$

Note that the frequency moments $\omega^{(m)}(Q)$, $m = 2, 4, \ldots$ are connected with the general relaxation parameters of the chain (8) $\Omega_1^2, \Omega_2^2, \ldots, \Omega_i^2, \ldots$ by the following relationship [18]:

$$\Omega_1^2 = \omega^{(2)}, \qquad \Omega_2^2 = \omega^{(4)}\omega^{(2)^{-1}} - \omega^{(2)}, \qquad \Omega_3^2 = \frac{\omega^{(6)}\omega^{(2)} - \omega^{(4)^2}}{\omega^{(4)}\omega^{(2)} - \omega^{(2)^3}}. \tag{13}$$

However, from the experimental point of view, the scattering intensity in IXS is proportional to the convolution between the experimental resolution function and a 'quantum

mechanical' dynamic structure factor $S_q(Q,\omega)$, affected by the detailed balance condition. The following approximation was used in works [6, 7]:

$$S_q(Q,\omega) \simeq \frac{\beta\hbar\omega}{1-\mathrm{e}^{-\beta\hbar\omega}} S(Q,\omega), \tag{14}$$

where $\beta = 1/k_B T$. This approximation connects $S_q(Q,\omega)$ with its classical counterpart $S(Q,\omega)$.

### *3.2. Non-Markovity parameter and its statistical spectrum*

Many authors have attempted to introduce a parameter to estimate memory effects in different relaxation processes [23–28]. These parameters are calculated with the help of different formulae and have various physical meanings. The non-Markovity parameter $\epsilon_1$, first appearing in [18], allows one to obtain valuable information concerning the non-Markovian properties of the wide range of relaxation processes in simple liquids.

Every relaxation process can be described by a characteristic timescale usually named the relaxation time, which is related to the corresponding TCF $M_i(t)$ in the chain of equations (8). Thus, a multilevel hierarchy of the relaxation times $\tau_i$ naturally appears. The relaxation times of the initial TCF $F(t)$ and of the first-order MF $M_1(t)$ are defined as follows:

$$\begin{aligned} \tau_0 &= \mathrm{Re}[\tilde{M}_0(0)], \qquad \tilde{M}_0(s) = \int_0^\infty \mathrm{d}t\, M_0(t)\mathrm{e}^{-st}, \\ \tau_1 &= \mathrm{Re}[\tilde{M}_1(0)], \qquad \tilde{M}_1(s) = \int_0^\infty \mathrm{d}t\, M_1(t)\mathrm{e}^{-st}. \end{aligned} \tag{15}$$

Then the dimensionless non-Markovity parameter will be defined by the following expression:

$$\epsilon_1 = \tau_0/\tau_1. \tag{16}$$

The non-Markovity parameter for any relaxation process can be calculated from equation (16), and depending on the value of $\epsilon_1$ different cases can be considered. The process is Markovian if $\epsilon_1 \to \infty$, quasi-Markovian when $\epsilon_1 > 1$ and finally non-Markovian as $\epsilon_1 \sim 1$.

The infinite set of values of non-Markovity parameters can be easily generalized to for the frequency-dependent case on the basis of definition (16) in the following way [19]:

$$\epsilon_i(\omega) = \left\{ \frac{\mu_{i-1}(\omega)}{\mu_i(\omega)} \right\}^{\frac{1}{2}}, \tag{17}$$

where $i = 1, 2, 3, \ldots$ and $\mu_i(\omega)$ is a power frequency spectrum for the $i$th relaxation level

$$\mu_j(\omega) = \left\{ \mathrm{Re} \int_0^\infty \mathrm{d}t\, \mathrm{e}^{\mathrm{i}\omega t} M_j(t) \right\}^2. \tag{18}$$

The meaning of the frequency-dependent generalization of the value of $\epsilon_1$ is the following. The definition of $\epsilon_1$ (equations (15) and (16)) is related to the time decay of the TCF $F(Q,t)$ and of the MF of the first order $M_1(Q,t)$, namely to the initial values of the corresponding Laplace transforms. The generalization introduced with equations (17) and (18) allows one to quantitatively estimate memory effects in the whole area of explored frequencies. It is clear from equations (16)–(18) that the parameter $\epsilon_0$ is only a limiting case of the frequency-dependent parameter $\epsilon_i(\omega)$:

$$\epsilon_i = \lim_{\omega \to 0} \epsilon_i(\omega). \tag{19}$$

The $i$-suffix indicates here the considered relaxation level.

### 3.3. Memory function approach

There are many different methods for the calculation of the density correlation function, $F(Q,t)$. In the majority of these approaches the closure of the infinite chain of the non-Markovian kinetic equations (8) is searched for. The easiest way to perform such a closure is to introduce a model MF. Typically, the $i$th-order MF can be reasonably well approximated by known model functions, such as exponential, Gaussian and hyperbolic secant [29–32]. The main limitation of this approach obviously lies in the absence of convincing justification for the above-mentioned ansatz on the MF form.

An alternative and successive method is based on Bogolubov's idea of the reduced description and the hierarchy of the relaxation times in liquids [33]. According to this approach, it is possible to hypothesize that on a certain relaxation level the timescale invariance (equiscaling) of the two nearest interconnected relaxation processes can exist. As a result, the relaxation time does not vary with transition from one relaxation level to another: on a given relaxation level there exist the invariance of timescales of the nearest relaxation processes, i.e.

$$M_{i+1}(t) \approx M_i(t). \tag{20}$$

The given expression is referred to as the first correlation approximation (FCA), successfully applied to describe different relaxation processes in liquids [18, 34–39]. Within this approximation, the relaxation phenomena under study are described through $M_0(t) = F(t), M_1(t), \ldots, M_{i-1}(t)$.

It is worthwhile to emphasize that the chain resulting from the approximations $M_1(t) \approx F(t)$, $M_2(t) \approx M_1(t), \ldots, M_{i+1}(t) \approx M_i(t)$ forms a full set. In this set, the solution can be obtained with the help of $M_i(t) \approx M_{i-1}(t)$ and it is just a specific case at approximation $M_{i+1}(t) \approx M_i(t)$. So, FCA of a higher order contains a wider spectrum of different solutions. In the case of approximate equality of the neighbouring general relaxation frequency parameters $\Omega_i^2$ and $\Omega_{i+1}^2$ the following relation is true: $M_{i+1}(t) \approx M_i(t) \approx M_{i-1}(t)$. In this way, the approximation for the MF of the $(i+1)$th order, $M_{i+1}(t) \approx M_i(t)$, transforms to the approximation for the MF of the $i$th order, $M_i(t) \approx M_{i-1}(t)$, at which more convenient calculations of the Laplace transform of the initial TCF are required (see appendix A). Thus, the timescales of relaxation processes on the $i$th level become invariant in this case.

The definition of the closure level is the crucial point of the theory. In order to describe one-particle and collective dynamics in INS spectra of liquid argon, neon, aluminium and others [18, 34, 35] the approximation for MFs of the second and the third orders was applied. To calculate $S(Q,\omega)$ for liquid caesium near its melting point an FCA modification method based on expressing the third-order MF in terms of the scaled second-order MF [16] was used.

From the previous discussion we see how the choice of the closure level of the relaxation chain can be based on the definition and the comparison of relaxation scales of the corresponding TCFs $\tau_0, \tau_1, \ldots, \tau_i, \ldots$ and of the general relaxation parameters $\Omega_1^2, \Omega_2^2, \ldots, \Omega_j^2$. The calculation of the first quantities $\tau_0$ and $\Omega_1^2$ is correct: the first can be easily defined from the experimental data, and $\Omega_1^2$ is simply deduced from its definition (9). Further, the parameter $\Omega_2^2$ is defined as

$$\begin{aligned} \Omega_2^2 &= \omega_2^2 - \Omega_1^2; \\ \omega_2^2 &= 3\Omega_1^2 S(Q) + \frac{N}{mV}\int \mathrm{d}\boldsymbol{r}\, g(r)[1-\cos(\boldsymbol{Q}\boldsymbol{r})]\nabla_l^2 u(r), \end{aligned} \tag{21}$$

whereas $\Omega_3^2$ has the following expression:

$$\Omega_3^2 = \frac{\omega_3^2\omega_2^2 - \omega_2^4}{\Omega_2^2},$$

$$\omega_3^2 = \frac{1}{\omega_2^2}\left\{15\left(\frac{k_BT}{m}\right)^2 Q^4 + \frac{k_BT}{m} Q^2 \frac{N}{mV}\int \mathrm{d}\boldsymbol{r}\, g(r)\nabla_l^2 u(r)\right.$$
$$+ 6\frac{k_BT}{m^2} Q \frac{N}{V}\int \mathrm{d}\boldsymbol{r}\, g(r)\nabla_l^3 u(r)\sin(\boldsymbol{Q}\boldsymbol{r}) \qquad (22)$$
$$+ 2\frac{N}{m^2V}\int \mathrm{d}\boldsymbol{r}\, g(r)[\nabla\nabla_l u(r)]^2[1-\cos(\boldsymbol{Q}\boldsymbol{r})] + \left(\frac{N}{mV}\right)^2 \int \mathrm{d}\boldsymbol{r}\,\mathrm{d}\boldsymbol{r}'\, g_3(\boldsymbol{r},\boldsymbol{r}')$$
$$\left.\times [1+\cos(\boldsymbol{Q}(\boldsymbol{r}-\boldsymbol{r}')) - \cos(\boldsymbol{Q}\boldsymbol{r}-\boldsymbol{Q}\boldsymbol{r}')](\nabla\nabla_l u(r))(\nabla'\nabla_l' u(r'))\right\}.$$

Here the suffix $l$ denotes the component parallel to $Q$, $g(r)$ is the radial distribution function, $g_3(\boldsymbol{r},\boldsymbol{r}')$ is the three-particle distribution function and $u(r)$ is the pair interparticle potential. Higher-order frequency parameters contain higher-order distribution functions. The expressions for these quantities are given in [40]. Higher-order relaxation times are calculated by means of frequency parameters of the corresponding order:

$$\tau_{i+1} = (\Omega_{i+1}^2\tau_i)^{-1}, \qquad i = 0, 1, 2, \ldots. \qquad (23)$$

So, the direct calculation of higher-order parameters is extremely time consuming [41, 42], and therefore not realistic [43]. Although there exist different approximations (for example, [44, 45]), the final results of these calculations contain appreciable numerical errors [46, 47].

Three variables (density, momentum density and energy density) are usually used in hydrodynamics to study the complete dynamics of the system. For the description of the mechanisms underlying both collective and single-particle motions at the microscopic level (one or two interparticle distances) in simple liquids these three variables are always sufficient, and they appear implicitly in $F(Q,t)$, $M_1(Q,t)$ and $M_2(Q,t)$. Generally, the relaxation times of these three variables can be substantially different, while the timescales level off and become invariant on higher levels (see appendix B).

It is known that the calculations of dynamic structure factor are performed very actively by MD simulation (see, for example, [14, 15]), where a realistic interatomic potential, i.e. a potential model able to reproduce structural properties, is chosen. Comparison of the results of these numerical investigations with the experimental data reveals a short-range and a fast-damped oscillatory form of interatomic potential in liquid alkali metals. For example, the Ashcroft pseudopotential (with a core radius 0.905 Å) is shown to be appropriate in treating liquid sodium [48] in contrast with liquid lithium, where it is totally invalid. Such behaviour of the ion–ion potential in liquid sodium reflects similarities with the scenario of electric field gradient (EFG) of NQR relaxation in liquid metals [49]. A microscopic theory of nuclear quadrupole relaxation in liquid metals is developed in [49] with use of the Zwanzig–Mori formalism. It is based on some experimental data showing a rapprochement of timescales for the MFs of EFG (the second derivative of interaction potential) and for the next (higher-order) MF. The underlying case has many similarities with the NQR scenario in liquid metals. Indeed, the third dynamical variable $W_3$ (see equation (B.6)) resembles an EFG in NQR theory. The next fourth dynamical variable $W_4$ (see equation (B.7)) corresponds to a local EFG current density. It was shown in papers [49] that the relaxation timescale of these variables in liquid metals is the same. From the above-mentioned it is clear that $S(Q,\omega)$ is very sensitive to the asymmetry of EFG of the ion–ion interaction and its relaxation in liquid. On the basis of the previous observations, it seems reasonable to use the closure (20) for the third relaxation level with $i = 3$.

So, an FCA of the following form for calculations of spectra $S(Q,\omega)$ in the whole wavevector range should be used:

$$M_4(Q,t) = M_3(Q,t) + h(Q,t). \tag{24}$$

The 'tail function' $h(Q,t)$ is entered here. This function provides a correction to the correlation approximation over the whole interval of times $t$ (and frequencies $\omega$). The equation (24) yields a close system of four equations instead of the chain (8), where the fourth equation has the following form:

$$\frac{\mathrm{d}M_3(Q,t)}{\mathrm{d}t} = -\Omega_4^2 \int_0^t \mathrm{d}\tau\, \{M_3(Q,\tau) + h(Q,\tau)\} M_3(Q,t-\tau). \tag{25}$$

Solving the system by the Laplace–Fourier (LF) transform we find the expression for the initial TCF

$$\begin{aligned}\tilde{F}(Q,\mathrm{i}\omega) = \{&2\Omega_2^2\Omega_4^2 + \omega^2(\Omega_3^2 - 2\Omega_4^2) + \mathrm{i}\omega\Omega_3^2[\Omega_4^4\tilde{h}^2(Q,\mathrm{i}\omega) \\ &+ 2\mathrm{i}\omega\Omega_2^2\tilde{h}(Q,\mathrm{i}\omega) - \omega^2 + 4\Omega_4^2]^{1/2} - \mathrm{i}\omega\Omega_3^2\Omega_4^2\tilde{h}(Q,\mathrm{i}\omega)\}\{\Omega_1^2(\Omega_3^2 - \omega^2) \\ &\times [\Omega_4^4\tilde{h}^2(Q,\mathrm{i}\omega) + 2\mathrm{i}\omega\Omega_4^2\tilde{h}(Q,\mathrm{i}\omega) - \omega^2 + 4\Omega_4^2]^{1/2} \\ &- (\Omega_1^2 - \omega^2)\Omega_3^2\Omega_4^2\tilde{h}(Q,\mathrm{i}\omega) + \mathrm{i}\omega(2\Omega_2^2\Omega_4^2 + 2\Omega_1^2\Omega_4^2 - 2\omega^2\Omega_4^2 \\ &- \Omega_1^2\Omega_3^2 + \omega^2\Omega_3^2)\}^{-1}.\end{aligned} \tag{26}$$

Here $\tilde{h}(Q,\mathrm{i}\omega)$ is the LF transform of the 'tail function' $h(Q,t)$. The relevant result for $S(Q,\omega)$ is presented in appendix C, which is directly obtained by means of FCA (24) and is true for the arbitrary values of $Q$ and $\omega$.

The expansion of $M_i(Q,t)$ at small times is given as (for more details, see appendix D)

$$M_i(Q,t) = 1 - \frac{1}{2!}\Omega_{i+1}^2 t^2 + \cdots. \tag{27}$$

Retaining the first two terms of the series for $i = 4$ the following approximate expression holds:

$$M_4(Q,t) \approx \mathrm{e}^{-\Omega_5^2 t^2/2}. \tag{28}$$

By the LF transform we obtain

$$\tilde{M}_4(Q,\mathrm{i}\omega) = \frac{1}{\Omega_5}\mathrm{e}^{-\omega^2/(2\Omega_5^2)}. \tag{29}$$

Similarly, for the fourth equation of (8), we obtain

$$\tilde{M}_3(Q,s) = \{s + \Omega_4^2\tilde{M}_4(Q,s)\}^{-1}. \tag{30}$$

Rewriting equation (24) in terms of (30) we obtain

$$\tilde{M}_4(Q,s) = \frac{1}{s + \Omega_4^2\tilde{M}_4(Q,s)} + \tilde{h}(Q,s). \tag{31}$$

After substitution of equations (29) and (31) we obtain

$$\tilde{h}(Q,\mathrm{i}\omega) = \frac{\Omega_4^4\mathrm{e}^{-3\omega^2/(2\Omega_5^2)} + \omega^2\Omega_5^2\mathrm{e}^{-\omega^2/(2\Omega_5^2)} - \Omega_4^2\Omega_5^2\mathrm{e}^{-\omega^2/(2\Omega_5^2)} + \mathrm{i}\omega\Omega_5^3}{\Omega_4^4\Omega_5\mathrm{e}^{-\omega^2/\Omega_5^2} + \omega^2\Omega_5^3}. \tag{32}$$

Since the third relaxation level takes on the properties of timescale invariance, the corresponding frequency parameters will also be approximately equal, $\Omega_5^2 \approx \Omega_4^2$ (see appendix A). Then $\tilde{h}(Q,s)$ may be written in the following form:

$$\tilde{h}(Q,\mathrm{i}\omega) = \frac{\mathrm{e}^{-\omega^2/(2\Omega_4^2)}(\omega^2 + \Omega_4^2\mathrm{e}^{-\omega^2/\Omega_4^2} - \Omega_4^2) + \mathrm{i}\omega\Omega_4}{\Omega_4\omega^2 + \Omega_4^3\mathrm{e}^{-\omega^2/\Omega_4^2}}. \tag{33}$$

However, this equation can be used in calculation only for a limited region of large frequencies ($\omega \geqslant 2\Omega_4$). From different experimental investigations [1] it is well known that the data for this frequency region are not available. On the other hand, the correction $\tilde{h}(Q, \mathrm{i}\omega)$ is negligible in this frequency range. Using equations (10) and (26) we finally obtain the expression for $S(Q, \omega)$

$$S(Q,\omega) = \frac{S(Q)}{2\pi}\Omega_1^2\Omega_2^2\Omega_3^2(4\Omega_4^2-\omega^2)^{\frac{1}{2}}\{\Omega_1^4\Omega_3^4 + \omega^2(-2\Omega_1^2\Omega_3^4+\Omega_1^4\Omega_4^2-\Omega_1^4\Omega_3^2+2\Omega_1^2\Omega_2^2\Omega_4^2-\Omega_1^2\Omega_2^2\Omega_3^2+\Omega_2^4\Omega_4^2) + \omega^4(\Omega_3^4-2\Omega_1^2\Omega_4^2+2\Omega_1^2\Omega_3^2-2\Omega_2^2\Omega_4^2+\Omega_2^2\Omega_3^2)+\omega^6(\Omega_4^2-\Omega_3^2)\}^{-1}. \tag{34}$$

## 4. Numerical calculations and discussion

We now apply the introduced formalism to the discussion of the experimental data for liquid sodium at the melting point ($T = 390$ K) in the range of wavevector from 1.5 to 14.6 $\mathrm{nm}^{-1}$ (see figure 2). Equation (34) was used to test the theory against the data. The static structure factor $S(Q)$-data are taken from [9] and are illustrated together with the Waseda data [50] in figure 1. From $S(Q)$ the quantity $\Omega_1^2$ is simply deduced by definition (9). Different kinds of approximation exist to calculate frequency parameters $\Omega_2^2$. For example, according [45], one can use the following equation:

$$\Omega_2^2 = \omega_l^2 - \Omega_1^2,$$
$$\omega_l^2 \simeq \frac{3Q^2}{m\beta} + \omega_E^2\left\{1 - \frac{3\sin(QR_0)}{QR_0} - \frac{6\cos(QR_0)}{(QR_0)^2} + \frac{6\sin(QR_0)}{(QR_0)^3}\right\}, \tag{35}$$

where parameter $\omega_E$ is the value of the order of the maximum phonon frequency in the solid [22]. However, this approximation is not suitable for some $Q$-regions. Alternatively, the $Q$-dependence of frequency $\omega_l$ is related to the generalized infinite-frequency velocity by [51]

$$c_\infty(Q) \equiv \frac{\omega_l(Q)}{Q} = \frac{\sqrt{\Omega_1^2+\Omega_2^2}}{Q}. \tag{36}$$

Therefore the values of $\Omega_2^2$ are easily expressible in terms of known values of $c_\infty(Q)$.

We report the quantities $\Omega_1^2$ and $\Omega_2^2$ (from equation (36)) in figure 3, along with $\Omega_{2apr}^2$, which is calculated with the help of the Hubbard approximation (35). The Einstein frequency $\omega_E$ is taken to be 16.2 $\mathrm{ps}^{-1}$ which was obtained by Rahman [54], whereas the values of $c_\infty(Q)$ are taken from [10]. It is clear from this figure that the frequency parameters $\Omega_1^2$ and $\Omega_2^2$ have a dispersive behaviour, with $\Omega_{2apr}^2$ showing strong deviations from $\Omega_2^2$. So, we use the parameter $\Omega_2^2$ to calculate expression (34). The frequency parameters $\Omega_3^2$ and $\Omega_4^2$ can also be calculated within different approximations, and the final result is usually affected by a large error [46, 47]. Consequently, we decided to leave the high-order frequency parameters $\Omega_3^2$ and $\Omega_4^2$ as adjustable parameters. In figure 4 we report the $Q$ dependence of relaxation parameters $\Omega_i^2$ with $i = 3$ and 4, which are necessary to reproduce the dynamic structure factor lineshapes at the selected closure level. Table 1 helps to present clearly the numerical values of all the relaxation parameters used in our calculations together with $\Omega_{2apr}^2$ obtained from approximation (35). These frequency parameters carry information about the microdynamics of the studied system (as noted above, they are determined by the pair distribution function $g(r)$, the pair interparticle potential $u(r)$, the higher-order distribution functions and so on). This is apparent from equations (21) and (22). On the other hand, kinetic theory holds that diverse microdynamic parameters such as viscosity coefficient, self-diffusion constant, thermal

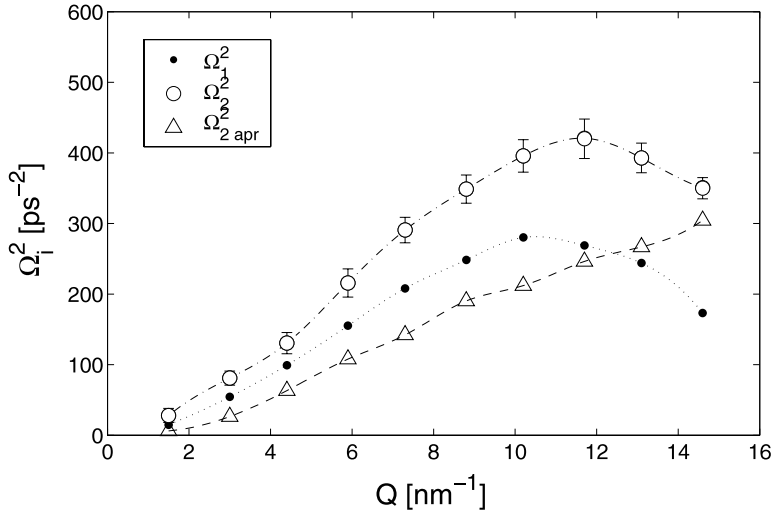


**Figure 3.** Wavevector dependence of relaxation parameters $\Omega_1^2(Q)$ calculated from its definition (full dots ●); $\Omega_{2apr}^2(Q)$ calculated from the well known approximation (35) and $\Omega_2^2$ as obtained from equation (36).

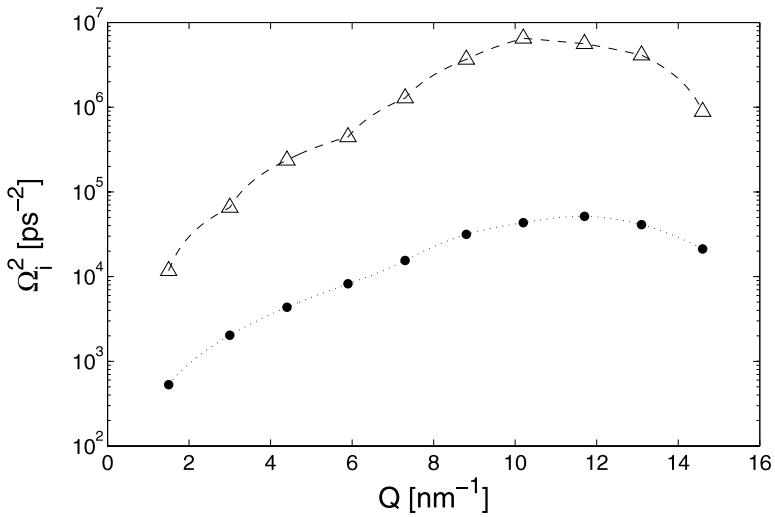


**Figure 4.** Wavevector dependence of relaxation parameters $\Omega_i^2$ ($i = 3$ and 4). The full circles (●) present $\Omega_3^2(Q)$ and open triangles (△) are the values of $\Omega_4^2(Q)$.

conductivity and others are expressed by $u(r)$, $g(r)$, $g_3(\boldsymbol{r}, \boldsymbol{r}')$ and other microscopic and statistical properties [22, 55–57].

The results for the dynamic structure factor $S(Q, \omega)$ for $Q$ values from 1.5 to 14.6 nm$^{-1}$, obtained by means of IXS [9], are shown in figure 5. It is clear from this figure that our theory is in a good agreement with the experimental data, and therefore it gives a satisfactory description of the microdynamics of molten sodium. In figure 6 we report the dynamic structure factor $S(Q, \omega)$ calculated from our theory for the 'low-$Q$' region, where it demonstrates the shift

**Table 1.** Numerical values of the relaxation parameters $\Omega_1^2$, $\Omega_2^2$, $\Omega_3^2$ and $\Omega_4^2$ used in equation (34) together with $\Omega_{2apr}^2$ at various values of $Q$.

| $Q$ (nm$^{-1}$) | $\Omega_1^2$ ($10^{24}$ s$^{-2}$) | $\Omega_2^2$ ($10^{24}$ s$^{-2}$) | $\Omega_3^2$ ($10^{26}$ s$^{-2}$) | $\Omega_4^2$ ($10^{26}$ s$^{-2}$) | $\Omega_{2apr}^2$ ($10^{24}$ s$^{-2}$) |
|---|---|---|---|---|---|
| 1.5 | 14.9 | $28 \pm 2$ | 5.3 | 117.26 | 6.2 |
| 3 | 54.25 | $81 \pm 3$ | 20.2 | 654.46 | 22.74 |
| 4.4 | 99.18 | $130.5 \pm 10$ | 43.5 | 2 364.9 | 63.24 |
| 5.9 | 155.21 | $215.7 \pm 12$ | 82.3 | 4 458.6 | 104.1 |
| 7.3 | 208 | $290.3 \pm 10$ | 154.95 | 12 816 | 128.17 |
| 8.8 | 248.32 | $348.7 \pm 11$ | 314.8 | 36 613 | 184.5 |
| 10.2 | 280.18 | $395.8 \pm 12$ | 434.3 | 65 108 | 211.97 |
| 11.7 | 268.9 | $420.7 \pm 18$ | 514.2 | 56 109 | 240.58 |
| 13.1 | 243.83 | $392.8 \pm 15$ | 410 | 41 169 | 266.81 |
| 14.6 | 173.05 | $350.63 \pm 9$ | 212.4 | 8 867.7 | 302.21 |

of the side peak positions. In figure 7 the dispersion of collective excitations $\omega_c(Q)$ obtained from the results of theory and experiment is presented. Again, the theory well reproduces the position of the collective excitation peaks.

To gain a better understanding of the origin of the collective excitations in the 'low-$Q$' region we introduced the non-Markovity parameter, which allows us to estimate the memory effects of different relaxation levels over the whole frequency range. We have calculated the first three points in the statistical spectrum of the frequency-dependent non-Markovity parameter $\epsilon_i(Q, \omega)$ by using equation (17) (see figure 8). It is worthwhile to underline the importance of the non-Markovity parameter $\epsilon_1(Q, \omega)$ as it does not depend on any specific theory. Let us now write $\tilde{F}(Q, \omega) = F'(Q, \omega) + iF''(Q, \omega)$ and $\tilde{M}_1(Q, \omega) = M_1'(Q, \omega) + iM_1''(Q, \omega)$, where $F'$ and $M_1'$, $F''$ and $M_1''$ are real and imaginary parts of corresponding TCFs. The relevant power spectra can be directly obtained from equations (17) and (18):

$$\mu_0(Q, \omega) = F'^2(Q, \omega),$$

$$\mu_1(Q, \omega) = M_1'^2(Q, \omega) = \frac{F'^2(Q, \omega)}{\Omega_1^4[F'^2(Q, \omega) + F''^2(Q, \omega)]^2}.$$

Consequently, the first non-Markovity parameter $\epsilon_1(Q, \omega) = [\mu_0(Q, \omega)/\mu_1(Q, \omega)]^{\frac{1}{2}}$ is determined by $\tilde{F}(Q, \omega)$, and by the first frequency parameter $\Omega_1^2$ only, which can be calculated with high accuracy from its definition (9).

As can be observed, the central and the side peaks in frequency dependence of the calculated parameter $\epsilon_1(Q, \omega)$ are observed precisely at the same frequencies as the one of $S(Q, \omega)$. Moreover, the inelastic peaks of $S(Q, \omega)$ start to vanish at $Q = 14.6$ nm$^{-1}$, and a flattening of the side peaks of parameter $\epsilon_1(Q, \omega)$ around the same $Q$-value is also observed. One can also notice that in the whole frequency region where collective excitations are well pronounced the parameter $\epsilon_1(Q, \omega)$ satisfies the condition $\epsilon_1(Q, \omega) \gtrsim 1$. Therefore, we can state with assurance that the microdynamics of molten sodium exhibits a pronounced non-Markovian nature of collective excitations in the 'low-$Q$' region. Notice that a similar correspondence between $S(Q, \omega)$ and $\epsilon_1(Q, \omega)$ spectra has been found in liquid caesium [17] too.

Finally, we also calculated the parameter $\epsilon_1(Q)$ on the basis of equations (15) and (16):

$$\epsilon_1(Q) = \Omega_1^2 \left[ \frac{\pi S(Q, \omega = 0)}{S(Q)} \right]^2.$$

The results, illustrated in figure 9, confirm again that the collective excitations of liquid sodium in the 'low-$Q$' region are exclusively non-Markovian.

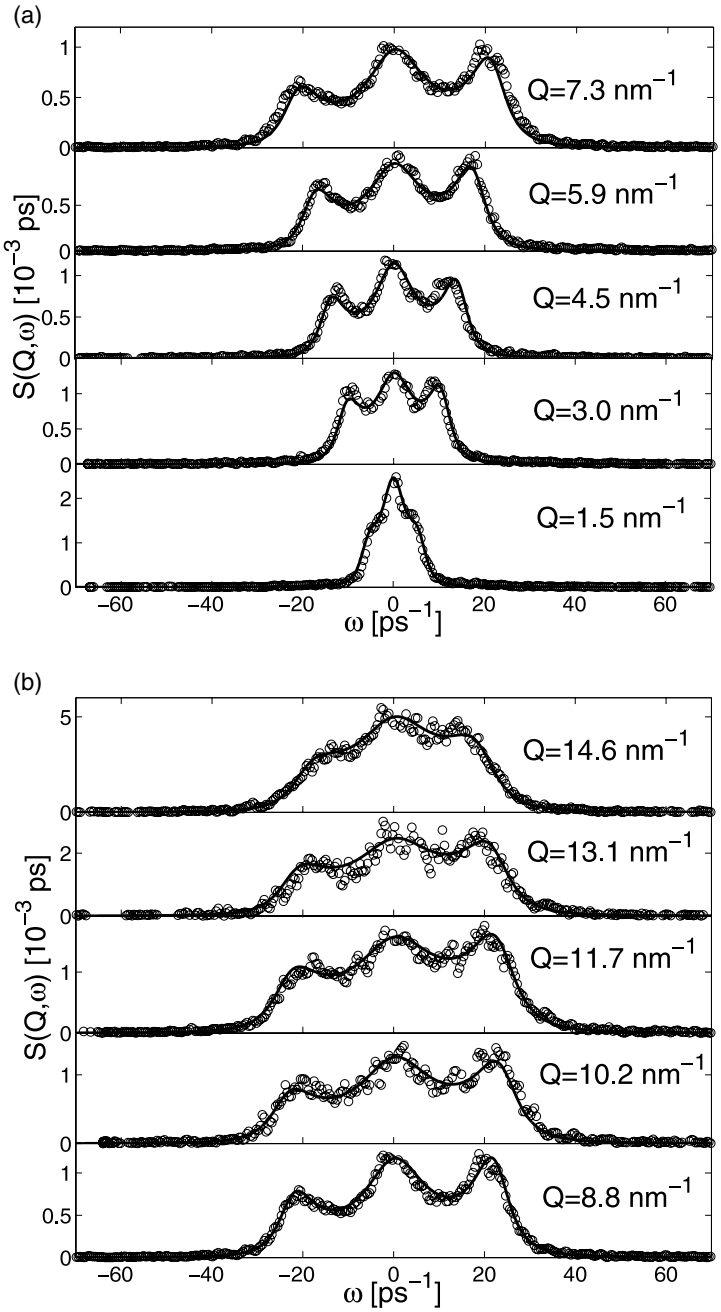


**Figure 5.** Theoretical (——) and experimental [9] (○) values of the dynamic structure factor $S(Q, \omega)$ of liquid sodium at $T = 390$ K and fixed values of wavevector $Q$. The theoretical lineshape has been modified to account for the quantum mechanical detailed balance condition and broadened for finite experimental resolution effects (see text).

## 5. Conclusion

In this work we have presented new evidence for the efficiency of the idea of timescale invariance (TSI idea) of relaxation processes applied to the specific case of molten sodium.

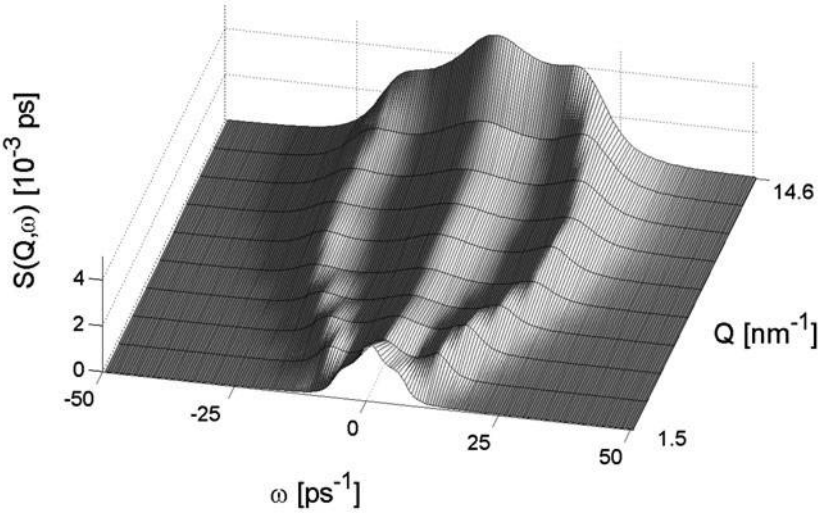


**Figure 6.** Dynamic structure factor calculated on the basis of our theory for liquid sodium at $T = 390$ K showing the change of side peak position for the 'low-$Q$' region.

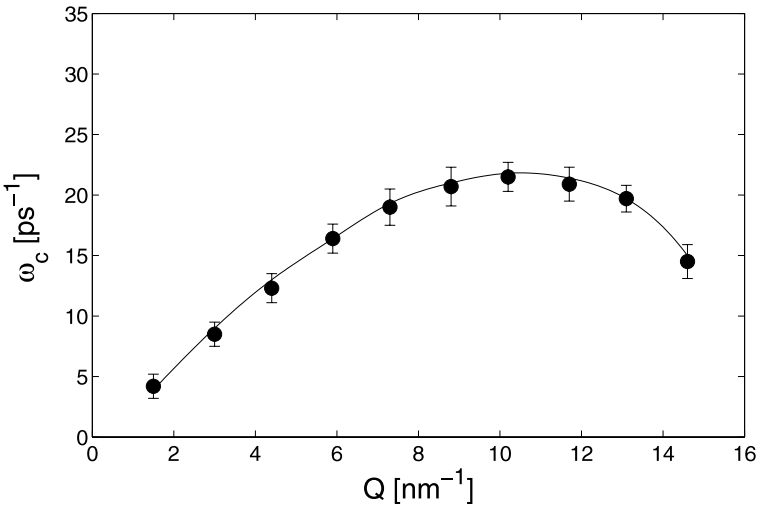


**Figure 7.** Dispersion relation, $\omega_c(Q)$, for liquid sodium at $T = 390$ K derived from the experimentally observed side peaks [9] (●) and our theory (——).

The dynamic structure factor of this system has been recently studied in the $Q$-region 1.5–14.6 nm$^{-1}$ by means of a very-high-energy-resolution IXS experiment, and the results have been interpreted within an MF formalism [10]. In this paper, starting from the TSI idea, we assumed that relaxation times of the third and the fourth relaxation levels are approximately equal to each other and therefore that the relevant timescales are invariant. Then we used the correlation approximation (24) for closure of the infinite chain of the non-Markovian kinetic equations (8). As a result, we obtained good agreement with the experiment in the whole range of wavevector $Q$. Notice that our theory does not contradict the viscoelastic model (see appendix E).

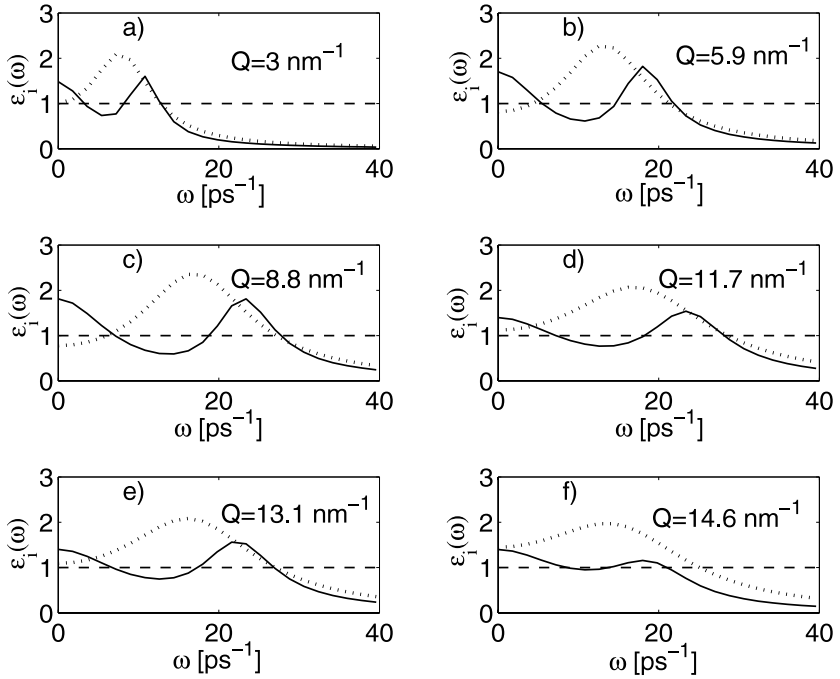


**Figure 8.** Frequency dependence of the non-Markovity parameter $\epsilon_i = \epsilon_i(\omega)$ at fixed values of $Q$; the solid curve (——) is related to $i = 1$; $(\cdots)$ corresponds to $i = 2$ and the broken line (— — —) reflects the values at $i = 4$. The parameter $\epsilon_3(\omega)$ has a descending curve for the whole wavevector range.

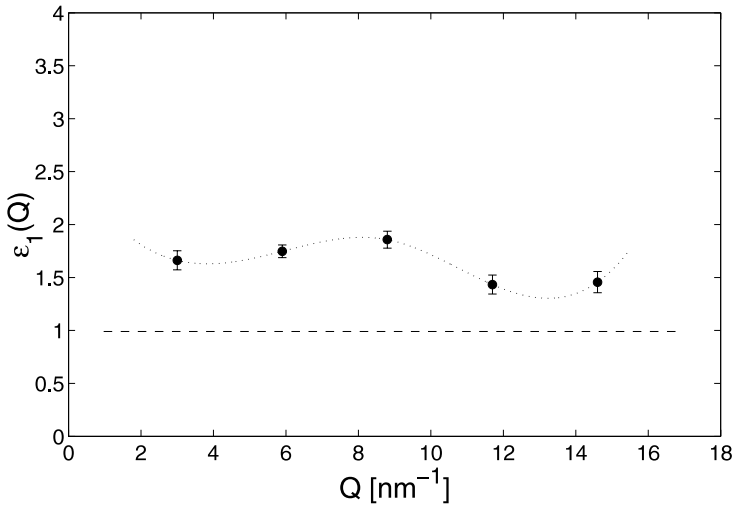


**Figure 9.** Non-Markovity parameter of the density fluctuations in liquid sodium for low values of the wavevector $Q$.

The frequency-dependent non-Markovity parameters $\epsilon_i(Q, \omega)$ ($i = 1, 2, 3$ and 4) were also calculated. In particular, we found that $\epsilon_1(Q, \omega)$, as well as in the case of liquid

caesium [17], has a frequency dependence similar to the one of the dynamic structure factor, with maxima occurring at the same frequencies. Our calculations have then established the non-Markov nature of collective excitations in a spatial range matching the interparticle distances.

The statistical theory of dynamical processes in liquids is closely related to Bogolubov's idea of hierarchy of relaxation times [58]. According to this idea, various timescales exist in liquids, and they are connected with specific characteristic relaxation processes. The theory of simple liquids should take these timescales into account and ensure smooth coupling of processes from one relaxation mode to another, as such a hierarchy has been experimentally reported in a wide range of relaxation phenomena in liquids: molecular light scattering [59, 60], dielectric relaxation [38], electronic spin, nuclear magnetic and quadrupole electric relaxation [33], inelastic neutron and x-ray scattering [1, 6, 7, 9, 10] and various transport and diffusion phenomena [61].

It must be emphasized that the idea of TSI and the idea of hierarchy do not contradict but mutually support each other. In our opinion the powerful combination of these two ideas forms a universal physical concept that should be taken into account for the description of relaxation processes in liquids.

Finally, we believe that theoretical approaches, such as the one we have presented here, may supply an important tool to interpret diverse IXS experiments on liquids.

## Acknowledgments

RMY and AVM acknowledge Professor A G Novikov and Dr V Yu Shurygin for stimulating discussions, and Dr L O Svirina for technical assistance. TS is grateful to U Balucani, E Pontecorvo and G Ruocco for useful suggestions and for manuscript revision. This work is partially supported by the Russian Humanitarian Science Fund (grant N 00-06-00005a) and the NIOKR RT Foundation (grant N 06-6.6-98/2001).

## Appendix A

Taking the LF transform of equations (8), we obtain equations of the form

$$\mathrm{i}\omega\tilde{M}_i(Q,z) - 1 = -\Omega_{i+1}^2\tilde{M}_{i+1}(Q,z)\tilde{M}_i(Q,z). \tag{A.1}$$

As a result of the FCA of the $(i)$th order MF, i.e., $M_i(Q,t) \approx M_{i-1}(Q,t)$, we obtain the next system of two equations

$$\mathrm{i}\omega\tilde{M}_i(Q,z-1) = \begin{cases} -\Omega_i^2\tilde{M}_i^2(Q,z), \\ -\Omega_{i+1}^2\tilde{M}_{i+1}(Q,z)\tilde{M}_i(Q,z). \end{cases} \tag{A.2}$$

After solving equations (A.2) we have

$$\tilde{M}_{i+1}(Q,z) = \frac{\Omega_i^2}{\Omega_{i+1}^2}\,\tilde{M}_i(Q,z). \tag{A.3}$$

So, if $\Omega_{i+1}^2 \approx \Omega_i^2$, then the expression $M_{i+1}(t) \approx M_i(t) \approx M_{i-1}(t)$ holds.

## Appendix B

The MF of $(i)$th order ($i = 0, 1, 2, \ldots$) in the general case is defined as

$$M_i(t) = \frac{\langle W_i(0)W_i(t)\rangle}{\langle |W_i(0)|^2\rangle}, \tag{B.1}$$

where $W_i(t)$ are dynamical variables of $i$th order, and relaxation parameters are defined by the following relation:

$$\Omega_{i+1}^2 = \frac{\langle |W_{i+1}(0)|^2 \rangle}{\langle |W_i(0)|^2 \rangle}. \tag{B.2}$$

The dynamical variables $W_i = W_i(0)$ have the following expressions ($|Q| \neq 0$):

$$W_0 = \frac{1}{V} \sum_{j=1}^{N} \mathrm{e}^{\mathrm{i}Qr_j}, \tag{B.3}$$

$$W_1 = \frac{1}{mV} \sum_{j=1}^{N} (m_j v_j^l) \mathrm{e}^{\mathrm{i}Qr_j}, \tag{B.4}$$

where the suffix $l$ denotes longitudinal, parallel to the $Q$-component.

$$W_2 = \frac{1}{mV} \sum_{j=1}^{N} \left\{ \frac{(m_j v_j^l)^2}{m} + \mathrm{i} \sum_{i>j=1}^{N} \nabla_j u(j,i) Q [1 - \mathrm{e}^{\mathrm{i}Q(r_i - r_j)}] \right\} - \frac{\Omega_1^2}{V} \sum_{j=1}^{N} \mathrm{e}^{\mathrm{i}Qr_j}, \tag{B.5}$$

$$\begin{aligned} W_3 = {} & \frac{1}{V} \sum_{j=1}^{N} \frac{(p_j Q)^3}{m^3} \mathrm{e}^{\mathrm{i}Qr_j} + \frac{2\mathrm{i}}{Vm^2} \sum_{i>j=1}^{N} (Q\nabla_j) u(i,j) \{ (p_j Q) \mathrm{e}^{\mathrm{i}Qr_j} - (p_i Q) \mathrm{e}^{\mathrm{i}Qr_i} \} \\ & + \sum_{i>j=1}^{N} \frac{p_j \nabla_j}{Vm^2} (Q\nabla_j) u(j,i) \{ \mathrm{e}^{\mathrm{i}Qr_j} - \mathrm{e}^{\mathrm{i}Qr_i} \} - (\Omega_1^2 + \Omega_2^2) W_1, \end{aligned} \tag{B.6}$$

and

$$\begin{aligned} W_4 = {} & \frac{1}{V} \sum_{j=1}^{N} \frac{(p_j Q)^4}{m^4} \mathrm{e}^{\mathrm{i}Qr_j} + \frac{3\mathrm{i}}{Vm^3} \sum_{i>j=1}^{N} (Q\nabla_j) u(j,i) [(p_j Q)^2 \mathrm{e}^{\mathrm{i}Qr_j} - (p_i Q)^2 \mathrm{e}^{\mathrm{i}Qr_i}] \\ & + \frac{2}{Vm^3} \sum_{i>j=1}^{N} p_j \nabla_j (Q\nabla_j) u(j,i) [(p_j Q) \mathrm{e}^{\mathrm{i}Qr_j} - (p_i Q) \mathrm{e}^{\mathrm{i}Qr_i}] \\ & - \frac{2}{Vm^2} \sum_{i>j=1}^{N} (Q\nabla_j)^2 u^2(j,i) [\mathrm{e}^{\mathrm{i}Qr_j} + \mathrm{e}^{\mathrm{i}Qr_i}] - \frac{\mathrm{i}}{Vm^3} \sum_{i>j=1}^{N} p_j^2 \nabla_j^2 (Q\nabla_j) \\ & \times u(j,i) [\mathrm{e}^{\mathrm{i}Qr_j} - \mathrm{e}^{\mathrm{i}Qr_i}] + \frac{\mathrm{i}}{Vm^2} \sum_{i>j=1}^{N} \nabla_j u(j,i) (\nabla_j - \nabla_i) (Q\nabla_j) u(j,i) \\ & \times [\mathrm{e}^{\mathrm{i}Qr_j} - \mathrm{e}^{\mathrm{i}Qr_i}] - (\Omega_1^2 + \Omega_2^2 + \Omega_3^2) W_2 - (\Omega_1^2 + \Omega_2^2) \Omega_1^2 W_0. \end{aligned} \tag{B.7}$$

So, the introduction of approximation (24) is related to a specific feature of liquid metals. In particular, it is connected with the short-range behaviour of ion–ion potential. One can see from the above-mentioned equations (B.1), (B.3)–(B.7) that time correlation of Fourier components of a local momentum density, local energy density and local energy current density occurs in MFs $M_1(t)$, $M_2(t)$ and $M_3(t)$, respectively. Space and momentum functions arise in appropriate dynamic variables, depending on position and momentum of molecules of liquids. The levelling of the relaxation timescale on the third and fourth levels occurs through the entanglement of these functions and due to the short-range character of the ion–ion interactions.

## Appendix C. The exact solution of the set of kinetic equations with the tail function for $M_4(t)$

Writing the 'tail function' at fixed $Q$ as $\tilde{h}(\omega) = h'(\omega) + \mathrm{i}h''(\omega)$, we obtain

$$S(Q,\omega) = \begin{matrix} S(Q) & \omega^3 A_3 + \omega^2 A_2 + \omega A_1 + A_0 \\ \pi & \omega^6 B_6 + \omega^5 B_5 + \omega^4 B_4 + \omega^3 B_3 + \omega^2 B_2 + \omega B_1 + B_0 \end{matrix}, \tag{C.1}$$

where

$$A_3 = (\Omega_3^2 - 2\Omega_4^2)(a^2+b^2)^{1/4}\cos(\varphi/2), \tag{C.2}$$

$$A_2 = (\Omega_3^2 - 2\Omega_4^2)(a_1^2+b_1^2)\cos(\varphi_1/2) + (2\Omega_4^2) - \Omega_3^2(a_2^2+b_2^2)^{1/4}\cos(\varphi_2/2) - \Omega_3^2\Omega_4^2[h'(\omega)(a^2+b^2)^{1/4}\sin(\varphi/2) - h''(\omega)(a^2+b^2)\cos(\varphi/2)], \tag{C.3}$$

$$A_1 = (2\Omega_2^2\Omega_4^2 + 2\Omega_1^2\Omega_4^2 - \Omega_1^2\Omega_3^2)(a^2+b^2)^{1/4}\cos(\varphi/2) + \Omega_3^2\Omega_4^2(a_1^2+b_1^2)^{1/4}[h''(\omega)\cos(\varphi_1/2) - h'(\omega)\sin(\varphi_1/2)] + \Omega_3^2\Omega_4^2(a_2^2+b_2^2)^{1/4}[h'(\omega)\sin(\varphi_2/2) - h''(\omega)\cos(\varphi_2/2)], \tag{C.4}$$

$$A_0 = -2\Omega_1^2\Omega_2^2\Omega_3^2\Omega_4^4 h'(\omega) + \Omega_1^2\Omega_3^2\Omega_4^2(a^2+b^2)^{1/4}[h'(\omega)\sin(\varphi/2) - h''(\omega)\cos(\varphi/2)] + 2\Omega_2^2\Omega_4^2(a_1^2+b_1^2)^{1/4}\cos(\varphi_1/2) - 2\Omega_2^2\Omega_4^2(a_2^2+b_2^2)^{1/4}\cos(\varphi_2/2), \tag{C.5}$$

$$B_6 = (2\Omega_4^2 - \Omega_3^2)^2, \tag{C.6}$$

$$B_5 = 2\Omega_3^2\Omega_4^2 h''(\omega)(\Omega_3^2 - 2\Omega_4^2), \tag{C.7}$$

$$B_4 = \Omega_3^4\Omega_4^2(h'^2(\omega) + h''^2(\omega)) + 4\Omega_2^2\Omega_4^2(\Omega_3^2 - 2\Omega_4^2) + 2\Omega_1^2(4\Omega_3^2\Omega_4^2 - 4\Omega_4^4 - \Omega_3^4), \tag{C.8}$$

$$B_3 = 4\Omega_2^2\Omega_3^2\Omega_4^4 h''(\omega) - 2(\Omega_3^2 - 2\Omega_4^2)[2\Omega_1^2\Omega_3^2\Omega_4^2 h''(\omega) - (a_1^2+b_1^2)^{1/4}\sin(\varphi_1/2) + (a_2^2+b_2^2)^{1/4}\sin(\varphi_2/2)], \tag{C.9}$$

$$B_2 = -2\Omega_1^2\Omega_3^4\Omega_4^4[h'^2(\omega) + h''^2(\omega)] + \Omega_1^4(2\Omega_4^2 - \Omega_3^2)^2 - 4\Omega_1^2\Omega_2^2\Omega_4^2(\Omega_3^2 - 2\Omega_4^2) + 4\Omega_2^4\Omega_4^4 + \Omega_1^4\Omega_3^4 + 2\Omega_3^2\Omega_4^2(a_1^2+b_1^2)^{1/4}[h'(\omega)\cos(\varphi_1/2) + h''(\omega)\sin(\varphi_1/2)] - 2\Omega_3^2\Omega_4^2(a_2^2+b_2^2)^{1/4}[h'(\omega)\cos(\varphi_2/2) + h''(\omega)\sin(\varphi_2/2)], \tag{C.10}$$

$$B_1 = 2\Omega_1^4\Omega_3^2\Omega_4^2 h''(\omega)(\Omega_3^2 - 2\Omega_4^2) - 4\Omega_1^2\Omega_2^2\Omega_3^2\Omega_4^2 + 2\Omega_1^2(a_2^2+b_2^2)^{1/4}\sin(\varphi_2/2)(\Omega_3^2 - 2\Omega_4^2) - 4\Omega_2^2\Omega_4^2(a_2^2+b_2^2)^{1/4} \times \sin(\varphi_2/2) + 2(a_1^2+b_1^2)^{1/4}\sin(\varphi_1/2)(4\Omega_2^2\Omega_4^2 - \Omega_1^2\Omega_3^2), \tag{C.11}$$

$$B_0 = \Omega_1^4\Omega_3^4\Omega_4^4(h'^2(\omega) + h''^2(\omega)) + (a_1^2+b_1^2)^{1/2} + (a_2^2+b_2^2)^{1/2} - 2(a_1^2+b_1^2)^{1/4}(a_2^2+b_2^2)^{1/4}[\sin(\varphi_1/2)\sin(\varphi_2/2) + \cos(\varphi_1/2)\cos(\varphi_2/2)] - 2\Omega_1^2\Omega_3^2\Omega_4^2 h'(\omega)[(a_1^2+b_1^2)^{1/4}\cos(\varphi_1/2) - (a_2^2+b_2^2)^{1/4}\cos(\varphi_2/2)] - 2\Omega_1^2\Omega_3^2\Omega_4^2 h''(\omega)[(a_1^2+b_1^2)^{\frac{1}{4}}\sin(\varphi_1/2) - (a_2^2+b_2^2)^{1/4}\sin(\varphi_2/2)], \tag{C.12}$$

$$a = \omega^2\Omega_3^4[\Omega_4^4 h'^2(\omega) + 4\Omega_4^2 - \Omega_4^4 h''^2(\omega)] - 2\omega^3\Omega_3^4\Omega_4^2 h''(\omega) - \omega^4\Omega_3^4, \tag{C.13}$$

$$b = 2\omega^2\Omega_3^4\Omega_4^2 h'(\omega)[\Omega_4^2 h''(\omega) + \omega] \tag{C.14}$$

with $\varphi = \arctan(b/a)$,

$$a_1 = \Omega_1^4\Omega_3^4[\Omega_4^4 h'^2(\omega) + 4\Omega_4^2 - \Omega_4^4 h''^2(\omega)] - 2\omega h''(\omega)\Omega_1^4\Omega_3^4\Omega_4^2 - \omega^2\Omega_1^4\Omega_3^4, \tag{C.15}$$

$$b_1 = 2h'(\omega)\Omega_1^4\Omega_3^4\Omega_4^2[\Omega_4^2 h''(\omega) + \omega] \tag{C.16}$$

with $\varphi_1 = \arctan(b_1/a_1)$ and

$$a_2 = \omega^4\Omega_3^4[\Omega_4^4 h'^2(\omega) + 4\Omega_4^2 - \Omega_4^4 h''^2(\omega)] - \omega^6\Omega_3^4 - 2\omega^5 h''(\omega)\Omega_3^4\Omega_4^2, \tag{C.17}$$

$$b_2 = 2\omega^4\Omega_3^4\Omega_4^2 h'(\omega)[\Omega_4^2 h''(\omega) + \omega] \tag{C.18}$$

with $\varphi_2 = \arctan(b_2/a_2)$.

## Appendix D

It is convenient to use Tauber theorems [62] about the restitution of the arbitrary function $f(t)$ when $t \to \infty$ or 0 by the properties of its Laplace image $\tilde{f}(s) = \int_0^\infty \mathrm{d}t\, \exp(-st) f(t)$ for the calculation of TCF. It is well known that asymptotic series are widely applied in approximate calculations of time functions at values of the arguments close to singular points $t_0$ ($0 \leqslant t_0 < +\infty$). The problem of approximation of the solution at $t \to t_0$ often arises when solving various tasks by the method of Laplace (Fourier) transformation. It is appropriate to use the expansion of the solution in asymptotic series in these cases. In this particular case, let us turn to the two important Tauber theorems [62].

The *first theorem* relates to the restitution $f(t)$ at $t \to \infty$ by the properties of its Laplace image $\tilde{f}(s)$. Let us assume that the function $\tilde{f}(s)$ possesses a finite number of singular points $s_\nu$ and it has the following form of the Laurent expansion in the neighbourhood of these points:

$$\tilde{f}(s) = \sum_{k=0}^{\infty} C_k^{(\nu)} (s - s_\nu)^{n_k^{(\nu)}}, \tag{D.1}$$

where $-\infty < n_0^{(\nu)} < n_1^{(\nu)} < n_2^{(\nu)} < \cdots < +\infty$. Then the function $f(t)$ at $t \to \infty$ has the form

$$f(t) = \sum_{\nu} \exp(s_\nu t) \sum_{k=0}^{\infty} C_k^{(\nu)} \{\Gamma(-n_k^{(\nu)})\}^{-1} t^{-(1+n_k^{(\nu)})}, \tag{D.2}$$

where we perform summation over all the singular points. For integer non-negative numbers $n_k^{(\nu)} = 0, 1, 2, \ldots$ we have $\{\Gamma(-n_k^{(\nu)})\}^{-1} = 0$. For example, for the first-order pole we have $n_k^{(\nu)} = 1$ and the corresponding contribution to the asymptotic behaviour of $f(t)$ is equal to $f_k^{(\nu)} = C_k^{(\nu)} \exp(s_\nu t)$.

The *second theorem* holds [62] that if the limit $\lim_{t \to +\infty} f(t)$ exists, then the next limit also exists,

$$\lim_{t \to +0} f(t) = \lim_{s \to \infty} \left[ s\, \tilde{f}(s) \right]. \tag{D.3}$$

The first Tauber theorem was widely used in statistical theory of nonequilibrium processes for quantum spin systems in classical liquids [33, 63]. In this work we use the second theorem to calculate the tail function $h(Q, t)$.

## Appendix E

As is well known, the following approximation for the time dependence of the normalized second-order MF $M_2(Q, t)$ is provided by the 'viscoelastic' model [22, 51]:

$$M_2(Q, t) = \mathrm{e}^{-t/\tau_l(Q)}. \tag{E.1}$$

It corresponds to the assumption that the third-order MF decays rapidly compared to the second-order MF. The idea of the approximate equality of timescales of $M_4$ and $M_3$, therefore, does not contradict the viscoelastic model, which can be seen as a lower-order truncation.

According to our theory, indeed, the Laplace transform of $M_2(Q, t)$ has the following exact form:

$$\tilde{M}_2(Q, s) = \frac{2\Omega_4^2(Q)}{s[2\Omega_4^2(Q) - \Omega_3^2(Q)] + \Omega_3^2(Q)\sqrt{s^2 + 4\Omega_4^2(Q)}}, \tag{E.2}$$

which can be obtained from equations (8) and (21) using the LF transform. Multiplying both the numerator and the denominator of equation (E.2) by $[2\Omega_4^2(Q) - \Omega_3^2(Q)]^{-1}$, we obtain

$$\tilde{M}_2(Q,s) = \frac{2\Omega_4^2(Q)[2\Omega_4^2(Q) - \Omega_3^2(Q)]^{-1}}{s + \Omega_3^2(Q)[2\Omega_4^2(Q) - \Omega_3^2(Q)]^{-1}\sqrt{s^2 + 4\Omega_4^2(Q)}}. \tag{E.3}$$

From the equation (E.3) one can see that if conditions $2\Omega_4^2(Q) \gg \Omega_3^2(Q)$ and $4\Omega_4^2(Q) \gg s^2$ are met then equation (E.3) can be written as

$$\tilde{M}_2(Q,s) = \frac{1}{s + \tau_l(Q)^{-1}}, \tag{E.4}$$

which corresponds to the viscoelastic model with a relaxation time $\tau_l^{-1}(Q) \approx \Omega_3^2/\Omega_4$.

The last equation, in fact, implies that the MF in this case will has an exponential time dependence of the same form as equation (E.1). The consequences of the viscoelastic approximation (E.1), (E.4) on the behaviour of the dynamic structure factor $S(Q,\omega)$ follow directly from the LF transforms of the first two equations of the chain (8). So, comparing this result in the $Q \to 0$ limit with the correct hydrodynamic expressions under isothermal conditions [55], the quantity $\Omega_2^2(Q)\tau_l(Q)$ can be identified with the damping of the sound mode, yielding $[\tau(Q \to 0)]^{-1} = nm[c_\infty^2 - c_0^2]/\eta_L$, where $n = N/V$, $c_0$ is the isothermal velocity of sound and $\eta_L$ is the longitudinal viscosity coefficient, which is related to the ordinary shear and bulk viscosities.

## References


[1] Copley J R D and Rowe J M 1974 *Phys. Rev.* A **9** 1656
Copley J R D and Rowe J M 1974 *Phys. Rev. Lett.* **32** 49
Chieux P, Dupuy-Philon J, Jal J F and Suck J B 1996 *J. Non-Cryst. Solids* **205–247** 370
Söderström O 1981 *Phys. Rev.* A **23** 785
Söderström O, Copley J R D, Suck J B and Dorner B 1980 *J. Phys. F: Met. Phys.* **10** L151
Dahlborg U and Larsson K E 1966 *Ark. Fys.* **33** 271
Larsson K E, Dahlborg U and Holmryd S 1960 *Ark. Fys.* **17** 369
Morkel C and Gläser W 1986 *Phys. Rev.* A **33** 3383
Stangl A, Morkel C, Balucani U and Torcini A 1996 *J. Non-Cryst. Solids* **205–207** 402
Verkerk P, De Jong P H K, Arai M, Bennington S M, Howells W S and Taylor A D 1992 *Physica* B **183** 834
Novikov A G, Savostin V V, Shimkevich A L, Yulmetyev R M and Yulmetyev T R 1996 *Physica* B **228** 312
[2] Bodensteiner T, Morkel C, Gläser W and Dorner B 1992 *Phys. Rev.* A **45** 5709
[3] Burkel E 1991 *Inelastic Scattering of X-Rays with Very High Energy Resolution* (Berlin: Springer)
[4] Masciovecchio C, Bergman U, Krisch M, Ruocco G, Sette F and Verbeni R 1996 *Nucl. Instrum. Methods* B **111** 181
Verbeni R, Sette F, Krisch M, Bergman U, Gorges B, Halcoussis C, Martel K, Masciovecchio C, Riois J F, Ruocco G and Sinn H 1996 *J. Synchrotron Radiat.* **3** 62
[5] Sinn H, Sette F, Bergman U, Halcoussis Ch, Krisch M, Verbeni R and Burkel E 1997 *Phys. Rev. Lett.* **78** 1715
[6] Scopigno T, Balucani U, Cunsolo A, Masciovecchio C, Ruocco G, Sette F and Verbeni R 2000 *Europhys. Lett.* **50** 189
Scopigno T, Balucani U, Ruocco G and Sette F 2000 *J. Phys.: Condens. Matter* **12** 8009
Scopigno T, Balucani U, Ruocco G and Sette F 2000 *Phys. Rev. Lett.* **85** 4076
[7] Scopigno T, Balucani U, Ruocco G and Sette F 2001 *Phys. Rev.* E **63** 011210
[8] Pilgrim W-C, Hosokawa S, Saggav H, Sinn H and Burkel E 1999 *J. Non-Cryst. Solids* **250–252** 96
[9] Scopigno T, Balucani U, Ruocco G and Sette F 2002 *Phys. Rev.* E **65** 031205
[10] Scopigno T 2001 *PhD Thesis* Universita' di Trento
[11] Hosokawa S, Kawakita Y, Pilgrim W-C and Sinn H 2001 *Phys. Rev.* B **63** 134205
[12] Hosokawa S *et al Proc. LAMI XI*
[13] Scopigno T *et al* 2002 *Phys. Rev. Lett.* **89** 255506
[14] Canales M, González L and Padró J A 1994 *Phys. Rev.* E **50** 3656

[15] Canales M and Padró J A 2000 *Phys. Rev.* E **63** 011207
[16] Sharma R K and Tankeshwar K 1997 *Phys. Rev.* E **55** 564
[17] Yulmetyev R M, Mokshin A V, Hänggi P and Shurygin V Yu 2001 *Phys. Rev.* E **64** 057101
Yulmetyev R M, Mokshin A V, Hänggi P and Shurygin V Yu 2002 *JETP Lett.* **76** 147
[18] Shurygin V Yu, Yulmetyev R M and Vorobjev V V 1990 *Phys. Lett.* A **148** 199
[19] Yulmetyev R, Hänggi P and Gafarov F 2000 *Phys. Rev.* E **62** 6178
[20] Mori H 1965 *Prog. Theor. Phys.* **33** 423
Mori H 1965 *Prog. Theor. Phys.* **34** 765
[21] Zwanzig R 1961 *Phys. Rev.* **124** 1338
Zwanzig R 1965 *Annu. Rev. Phys. Chem.* **16** 67
[22] Copley J R D and Lovesey S W 1975 *Rep. Prog. Phys.* **38** 461
[23] Egelstaff P A 1962 *Adv. Phys.* **11** 203
[24] Olemskoi A I 2001 *Usp. Fiz. Nauk* **171** 503 (in Russian)
[25] Brinati J R, Mizrahi S S and Prataveria G A 1994 *Phys. Rev.* A **50** 3304
Brinati J R, Mizrahi S S and Prataveria G A 1995 *Phys. Rev.* A **52** 2804
[26] Fulinski A, Grzywna Z, Mellor I, Siwy Z and Usherwood P N 1998 *Phys. Rev.* E **58** 919
Hänggi P and Jung P 1995 Colored noise in dynamical systems *Advances in Chemical Physics* vol LXXXIX, ed I Prigogin and S A Rice (New York: Wiley) pp 239–326
Fulinski A 1998 *Acta Phys. Pol.* B **29** 1523
[27] Oerding K, Cornell S J and Bray A J 1997 *Phys. Rev.* E **56** R25
Oerding K and van Wijland F 1998 *J. Phys. A: Math. Gen.* **31** 7011
[28] Teichler H 1996 *Phys. Rev.* E **76** 62
Teichler H 1992 *Phys. Status Solidi* b **172** 325
Teichler H 1997 *Defect and Diffusion Forum* vols 143–147 (Scitec) pp 717–22
[29] Yoshida F and Takeno S 1989 *Phys. Rep.* **173** 301
[30] Hoheisel C 1990 *Comput. Phys. Rep.* **12** 29
[31] Tankeshwar K, Dubey G S and Pathak K N 1988 *J. Phys. C: Solid State Phys.* **21** L811
[32] Tankeshwar K, Pathak K N and Ranganathan S 1990 *Phys. Chem. Liq.* **22** 75
[33] Yulmetyev R M 1977 *Teor. Mat. Fiz.* **30** 264
[34] Shurygin V Yu and Yulmetyev R M 1992 *Zh. Eksp. Teor. Fiz.* **102** 852
[35] Shurygin V Yu and Yulmetyev R M 1989 *Zh. Eksp. Teor. Fiz.* **96** 938
Shurygin V Yu and Yulmetyev R M 1990 *Teor. Mat. Fiz.* **83** 223
Shurygin V Yu and Yulmetyev R M 1989 *Phys. Lett.* A **135** 311
Shurygin V Yu and Yulmetyev R M 1989 *Phys. Lett.* A **141** 196
[36] Yulmetyev R M and Khusnutdinov N R 1994 *J. Phys. A: Math. Gen.* **27** 5363
Yulmetyev R M, Galeev R I and Yulmetyev T R 1994 *Physica* A **212** 26
Yulmetyev R M, Galeev R I and Shurygin V Yu 1995 *Phys. Lett.* A **202** 258
Yulmetyev R M and Khusnutdinov N R 1995 *Teor. Mat. Fiz.* **105** 292
[37] Gburski Z 1985 *Chem. Phys. Lett.* **115** 236
[38] Pasterny K and Kocot A 1987 *Chem. Phys. Lett.* **139** 295
[39] Galeev R I, Shurygin V Yu and Yulmetyev R M 1991 *Ukr. Fiz. Zh.* **36** 396 (in Russian)
[40] Bansal R and Pathak K N 1974 *Phys. Rev.* A **9** 2773
[41] Rosenfeld Y, Levesque D and Weis J-J 1990 *J. Chem. Phys.* **92** 6818
[42] Baranyai A and Evans D J 1989 *Phys. Rev.* A **40** 3817
[43] Kambayashi Sh and Kahl G 1992 *Phys. Rev.* A **46** 3255
[44] Machida M and Murase C 1973 *Prog. Teor. Phys.* **50** 1
[45] Hubbard J and Beeby J L 1969 *J. Phys. C: Solid State Phys.* **2** 556
[46] Shurygin V Yu and Yulmetyev R M 1990 *Metallofizika* **12** 55 (in Russian)
[47] Ebbsjo I, Kinell T and Waller I 1980 *J. Phys. C: Solid State Phys.* **13** 1865
[48] Ishitobi M and Chihara J 1992 *J. Phys.: Condens. Matter* **4** 3679
[49] Yulmetyev R M 1968 *Izvestija Vuzov Fizika* vol 8 (Russia: Tomsk) p 28
Yulmetyev R M 1996 *J. Struct. Chem.* **7** 841
Yulmetyev R M 1966 *Sov. Phys.–JETP* **51** 1090
Yulmetyev R M 1984 *Acta Phys. Pol.* A **65** 25
[50] Waseda Y 1980 *The Structure of Non-Crystalline Materials: Liquids and Amorphous Solids* (New York: McGraw-Hill)
[51] Balucani U, Ruocco G, Torcini A and Vallauri R 1993 *Phys. Rev.* E **47** 1677
[52] Michler E, Hahn H and Schofield P 1977 *J. Phys. F: Met. Phys.* **7** 869

[53] Dubey G S, Chaturvedi D K and Bansal R 1979 *J. Phys. C: Solid State Phys.* **12** 1997
[54] Rahman A 1974 *Phys. Rev. Lett.* **32** 52
[55] Balucani U and Zoppi M 1983 *Dynamics of the Liquid State* (Oxford: Clarendon)
[56] Boon J P and Yip S 1980 *Molecular Hydrodynamics* (New York: McGraw-Hill)
[57] Hansen J P and McDonald 1986 *Theory of Simple Liquids* (New York: Academic)
[58] Bogolubov N N 1946 *Problemy Dynamicheskoy Teorii v Statisticheskoi Fizike* (Moscow: GIFML)
[59] Patkowski A, Fischer E W, Steffen W, Gläser H, Baumann M, Ruths T and Meier G 2001 *Phys. Rev.* E **63** 061503
[60] Bunten R A J, Mc Greevy R L, Mitchell E W J, Raptis C and Walker P J 1984 *J. Phys. C: Solid State Phys.* **17** 4705
[61] Berg R F, Moldover M R and Zimmerli G A 1999 *Phys. Rev. Lett.* **82** 920
Berg R F, Moldover M R and Zimmerli G A 1999 *Phys. Rev.* E **60** 4079
Cutillas S and Liu J 2001 *Phys. Rev.* E **63** 061503
[62] Pailey R E C and Wiener N 1934 *Fourier Transforms in the Complex Domain* (New York: American Mathematical Society)
Ditkin V A and Prudnikov A P 1975 *Operation Calculus* (Moscow: High Education)
Markushevich A I 1950 *Theory of Analytic Functions* (Moscow: Gostechizdat)
[63] Yulmetyev R M, Shurygin V Yu and Khusnutdinov N R 1999 *Acta Phys. Pol.* B **30** 881